doi:10.1093/brain/awn334 Brain 2009: 132; 465–481 | 465

BRAIN
A JOURNAL OF NEUROLOGY

Myelin-mediated inhibition of oligodendrocyte precursor differentiation can be overcome by pharmacological modulation of Fyn-RhoA and protein kinase C signalling

Alexandra S. Baer,[1,*] Yasir A. Syed,[1,*] Sung Ung Kang,[2,*] Dieter Mitteregger,[1] Raluca Vig,[2] Charles ffrench-Constant,[3] Robin J. M. Franklin,[4] Friedrich Altmann,[5] Gert Lubec[2] and Mark R. Kotter[1,6]

1 Department of Neurosurgery, Medical University Vienna, Vienna, Austria
2 Department of Pediatrics, Medical University Vienna, Vienna, Austria
3 MS Society/University of Edinburgh Centre for Translational Research, Centre for Inflammation Research, The Queen's Medical Research Institute, Edinburgh, UK
4 Cambridge Centre for Brain Repair and Department of Veterinary Medicine, University of Cambridge, Cambridge, UK
5 University of Natural Resources and Applied Life Sciences Vienna, Vienna, Austria
6 Department of Neurosurgery, Georg-August University, Goettingen, Germany

*These authors contributed equally to this work.

Correspondence to: Dr Mark R. Kotter,
Max Planck Institute for Experimental Medicine and
Department of Neurosurgery,
Georg-August University Goettingen,
37075 Goettingen, Germany
E-mail: mark.kotter@med.uni-goettingen.de

Abstract

Failure of oligodendrocyte precursor cell (OPC) differentiation contributes significantly to failed myelin sheath regeneration (remyelination) in chronic demyelinating diseases. Although the reasons for this failure are not completely understood, several lines of evidence point to factors present following demyelination that specifically inhibit differentiation of cells capable of generating remyelinating oligodendrocytes. We have previously demonstrated that myelin debris generated by demyelination inhibits remyelination by inhibiting OPC differentiation and that the inhibitory effects are associated with myelin proteins. In the present study, we narrow down the spectrum of potential protein candidates by proteomic analysis of inhibitory protein fractions prepared by CM and HighQ column chromatography followed by BN/SDS/SDS–PAGE gel separation using Nano-HPLC-ESI-Q-TOF mass spectrometry. We show that the inhibitory effects on OPC differentiation mediated by myelin are regulated by Fyn-RhoA-ROCK signalling as well as by modulation of protein kinase C (PKC) signalling. We demonstrate that pharmacological or siRNA-mediated inhibition of RhoA-ROCK-II and/or PKC signalling can induce OPC differentiation in the presence of myelin. Our results, which provide a mechanistic link between myelin, a mediator of OPC differentiation inhibition associated with demyelinating pathologies and specific signalling pathways amenable to pharmacological manipulation, are therefore of significant potential value for future strategies aimed at enhancing CNS remyelination.

Received March 5, 2008. Revised September 7, 2008. Accepted November 12, 2008

Keywords: adult stem/precursor cells; oligodendrocyte; differentiation; myelin inhibitors; intracellular signalling; multiple sclerosis; remyelination

Abbreviations: MARCKS = Myristoylated, alanine-rich C-kinase substrate; MBP = myelin basic protein; MPEs = myelin protein extracts; OPC = oligodendrocyte precursor cells; PKC = protein kinase C; PLL = polylysine; 3DE = Three dimensional electrophoresis

Introduction

It is well established that cell populations in the adult CNS exist which are able to give rise to cells of all major cell lineages including neurons, oligodendrocytes and astrocytes (Alvarez-Buylla and Lois, 1995; Horner *et al*., 2000; Nunes *et al*., 2003). Although the ability of these cells to replace lost neurons is relatively poor their ability to replace oligodendrocytes (and hence remyelinate demyelinated axons) can be very efficient in both experimental models and sometimes in clinical disease (Patrikios *et al*., 2006; Patani *et al*., 2007; Blakemore and Franklin, 2008). Remyelination in the CNS is mediated by a multipotent adult stem/precursor cell population traditionally referred to as oligodendrocyte precursor cells (OPCs) (ffrench-Constant and Raff, 1986; Wolswijk and Noble, 1989; Gensert and Goldman, 1997; Carroll *et al*., 1998; Sim *et al*., 2002). Although remyelination can be efficient it often fails in clinical disease for reasons that are not fully understood (Franklin, 2002). The chronic demyelination that follows is associated with axonal loss, so providing a possible mechanism for progressive disability in patients suffering from diseases in which chronic demyelination occurs of which the most important is multiple sclerosis. Several lines of evidence both experimental (Woodruff *et al*., 2004; Foote and Blakemore, 2005) and clinical (Wolswijk, 1998, 2002; Chang *et al*., 2000; Totoiu and Keirstead, 2005; Kuhlmann *et al*., 2008) point to the failure of OPC differentiation as a major cause of remyelination failure. Indeed, regulation of OPC differentiation in remyelination represents an attractive model for the more general stem cell medicine challenge of inducing differentiation of repair cells from adult neural stem/precursor cells.

A possible explanation for the failure of OPC differentiation in multiple sclerosis is the presence of inhibitors within demyelinated lesions. A number of potential inhibitors have been proposed including axonal PSA-NCAM in chronically demyelinated lesions (Charles *et al*., 2002), astrocytic hyaluronan (Back *et al*., 2005) and notch-jagged (John *et al*., 2002) signalling, although these are not always supported by functional studies in animals models (Stidworthy *et al*., 2004). We have previously shown that myelin debris accumulating in lesions as a result of demyelination exerts a powerful inhibitory effect on OPC differentiation unless it is cleared by phagocytes (Kotter *et al*., 2006). With ageing, the efficiency of myelin debris removal decreases (Ibanez *et al*., 2004) and this may contribute to the impairment in OPC differentiation that underlies the age-associated decline in remyelination efficiency (Sim *et al*., 2002; Woodruff *et al*., 2004).

In this study, we identified potential protein inhibitors by column-chromatography based purification of inhibitory fractions followed by 3D gel electrophoresis and Nano-HPLC-ESI-Q-TOF mass spectrometry. We explored the cell intrinsic mechanisms by which myelin inhibits OPC differentiation in order to identify pathways that can be pharmacologically modulated and hence used as potential remyelination-enhancing therapies. We address the hypothesis that myelin-mediated inhibition of OPC differentiation is mediated by (i) Src-family (Fyn-1)–RhoA-ROCK-II signalling or (ii) protein kinase C (PKC) pathway signalling. By assessing the activation of key molecules of both pathways, we provide evidence of a direct involvement of Src family kinase Fyn and RhoA in mediating the inhibitory effects as well as a modulation of PKC signalling. Our results demonstrate that inhibition of either ROCK-II or PKC is able to induce OPCs differentiation in the presence of myelin thus providing a mechanism which could be of significant therapeutic value.

Materials and methods

Preparation and purification of OPC

Primary cultures of OPCs were isolated from P0 to P2 neonatal Sprague-Dawley rat forebrains following a standard protocol (McCarthy and de Vellis, 1980) that we have adapted for our purposes (Syed *et al*., 2008). In brief, hemispheres were stripped free of meninges, after a digestion step the cells were plated into cell culture flasks and mixed glia cultures were grown for ~10 days in DMEM medium supplemented with 10% FCS at 37°C and 7.5% CO_2. To remove the loosely attached microglia, the flasks were shaken for 1 h at 260 r.p.m. on an orbital shaker before being shaken at 260 r.p.m. overnight to dislodge the loosely attached oligodendrocyte precursors. OPCs were further purified from contaminating microglia by a differential adhesion step. Subsequently, OPCs were plated onto polylysine (PLL)-coated or substrate coated dishes. To maintain cells at an early precursor stage PDGF-AA (Pepro Tech, Rocky Hill, NJ, USA) and FGF (Pepro Tech) were added (10 ng/ml) to SATOs medium. To induce differentiation, cells were incubated in SATOs medium supplemented with 0.5% FCS. The purity of each culture was monitored following OPC purification by immunocytochemistry and only cultures with >94% purity were used. Minor contaminations of microglia, that can be detected by isolectin staining and which amount to 4–5% of the cells, astrocytes (detectable by GFAP) and fibroblasts with distinct morphology and which account for ~1–2% of the cells, were present in the cultures.

Preparation of myelin membrane substrates and myelin protein extracts

Myelin was purified by two rounds of discontinuous density gradient centrifugation and osmotic disintegration (Norton and Poduslo, 1973). Total brains of young Sprague-Dawley rats were homogenized mechanically in ice-cold 0.32 M sucrose using a mechanical blender (Ultra-Turrax; IKA, T18 basic, Germany). Sucrose was dissolved in sterile 2.5 mM Tris/HCl, pH 7.0, to form 0.25, 0.32 and 0.88 M solutions. The homogenized brains were diluted to a final 0.25 M sucrose solution and pelleted in an ultra-centrifuge (55 000 *g*, 4°C, 15 min). The pellet was re-suspended in 0.88 M sucrose solution and overlaid

with 0.25 M sucrose. After an ultracentrifugation step (100 000 *g*, 4°C, 1 h), the interface was collected and washed in 30 ml of distilled H_2O (55 000 *g*, 4°C, 10 min). The pellet was re-suspended in dH_2O and incubated for 60 min on ice for osmotic disintegration. After centrifugation (55 000 *g*, 4°C, 10 min), the flotation step was repeated. The interface was collected and washed twice in dH_2O (55 000 *g*, 4°C, 10 min), and the pellet was stored at –80°C until isolation of myelin protein extracts (MPEs).

To prepare MPE the pellets were resuspended in 1% *N*-octyl β-D-glucopyranoside, 0.2 M Sodiumphosphate pH 6.8, 0.1 M Na_2SO_4 and 1 mM EDTA and incubated at 23°C for 2 h. Following an ultracentrifugation step (100 000 *g*, 18°C, 30 min) the supernatants were collected and stored at –20°C until further usage (Kotter *et al*., 2006; Syed *et al*., 2008).

Isolation of liver membrane fractions

Sucrose (0.85 and 1.23 M) in 2.5 mM Tris/HCl was prepared as outlined above. The liver of a young adult Sprague-Dawley rat was extracted and homogenized in 0.85 M sucrose (using an Ultra-Turrax). The homogenate was layered onto a 1.23 M sucrose solution. After centrifugation (100 000 *g*, 4°C, 1 h) the interface was collected and washed in dH_2O (55 000 *g*, 4°C, 10 min). Finally, the pellet was resuspended in an equal volume of 1× PBS containing 1% octyglucoside and 1 mM EDTA. After incubation at 25°C for 2 h in a shaker the sample was ultracentrifuged at 100 000 *g* for 30 min and finally, the supernatant was stored at –20°C until further use. The protein concentration was estimated by BCA assay (Pierce, Rockford, IL, USA) (Kotter *et al*., 2006).

Chromatography column based separation of inhibitory myelin protein fractions

About 50 ml of the MPE (~1 mg/ml) were filtered through a 0.22 µ Millipore membrane filter. The filtrate was desalted and concentrated using Amicon ultrafiltration cell (Millipore, Billerica, MA, USA; membrane diameter 44.5 mm; cut off 10 000 Da) with 50 mM sodium acetate (pH4). This step was repeated three times to ensure that the sample was maximally desalted. The concentrated and desalted lysate was subsequently loaded on a CM column (Econo-Pac CM cartridges, 1 ml, Biorad, Hercules, CA, USA). Column chromatography was performed using an FPLC System with a built in detector (Pharmacia Fine Chemicals, GE Healthcare, Bucks. UK). The injection volume was 10 ml; 50 mM sodium acetate buffer containing 1% octlyglucoside (mobile phase A) was used as washing buffer and 1 M NaCl containing 1% octylglucoside (mobile phase B) was used as elution buffer. The following chromatographic gradients were applied: 0% B for 15 min, 0–70% B, hold with 70% B for 10 min followed by a wash with A for 10 min. The flow rate used was 2 ml/min, the fraction size 1 ml/min and sensitivity of the detector was 1 U at a wavelength of 280 nm.

The non-binding fractions and the binding fractions were pooled together separately and assessed for inhibitory activity on OPC differentiation using the *in vitro* substrate assay outlined below. Repeat experiments demonstrated that the inhibitory effects on OPC differentiation were associated with the nonbinding fraction of the CM column.

To further eliminate proteins with non-inhibitory activity, the inhibitory non-binding fraction was concentrated and the buffer exchanged to a 0.1 M Tris–Cl buffer containing 1% octlylglucoside (pH 8). The concentrate was subsequently loaded on an anion exchange EconoPac High Q cartridge (1 ml; Bio-Rad) and coupled to the FPLC system (GE Healthcare UK Ltd, Little Chalfont, Buckinghamshire, UK). 0.1 M Tris–Cl containing 1% octylglucoside was used as washing buffer (Mobile phase A). The binding fraction was eluted using 1 M NaCl in 0.1 M Tris–Cl containing 1% octylglucoside (Mobile Phase B). The injection volume was 10 ml. The reaction conditions were as follows: 0% B in 5 min and 0–100% B in 10 min, 100% B for 10 min and washing with A for 5 min. The flow rate was maintained at 2 ml/min at 25°C. The detection wavelength was 280 nm and sensitivity set at 1 U.

The resulting binding and non-binding fractions were again pooled separately. When tested for their inhibitory effects the inhibitory activity was associated with the binding fraction. The pooled binding fractions were further concentrated and the buffer exchanged to a buffer composed of 250 mM 6-aminocaproic acid, 25 mM Bis–Tris, pH 7.0 using Amicon ultra centrifugal filter devices.

One dimensional electrophoresis: BN-PAGE

60 µl of purified inhibitory myelin protein fractions (~2 µg/µl) was added to 10 µl of G250 solution [5% (w/v) Coomassie G250 in 10 mM 6-aminocaproic acid] and loaded onto the gel. BN-PAGE (Wittig *et al*., 2006) was performed in a PROTEAN II xi Cell (BioRad, Germany) using a 4% stacking and a 5–13% separating gel. The gel buffer contained 250 mM 6-aminocaproic acid, 25 mM Bis-Tris, pH 7.0; the cathode buffer 50 mM Tricine, 15 mM Bis-Tris, 0.05% (w/v) Coomassie G250, pH 7.0; and the anode buffer 50 mM Bis-Tris, pH 7.0. For electrophoresis, the voltage was set to 70 V for 2 h, and was increased to 250 V (10 mA/gel) until the dye front reached the bottom of the gel. BN-PAGE gels were cut into small pieces of ~1–3 cm depending on the intensity of protein bands for the BN/SDS/SDS–PAGE three dimensional electrophoresis (3DE).

Three dimensional electrophoresis: BN/SDS/SDS–PAGE

The experimental procedures and advantages of BN/SDS/SDS–PAGE (3DE) are summarized in Kang *et al*. (2008). Briefly, 1–3 cm gel pieces from BN-PAGE were soaked for 2 h in a solution of 1% (w/v) SDS and 1% (v/v) 2-mercaptoethanol. Gel pieces were then rinsed twice with SDS–PAGE electrophoresis buffer [25 mM Tris–HCl, 192 mM glycine and 0.1% (w/v) SDS; pH 8.3], then the gel pieces were placed onto the wells. 2DE-SDS–PAGE was performed in PROTEAN II xi Cell using a 4% stacking and a 6–13% separating gel for BN/SDS–PAGE (2DE). Electrophoresis was carried out at 25°C with an initial current of 70 V (during the first hour). The voltage was then set to 100 V for the next 12 h (overnight), and increased to 200 V until the bromophenol blue marker moved 17 cm from the top of separation gel.

2DE gels were cut again into lanes and gel strips from each lane were soaked for 20 min in a solution of 1% (w/v) SDS and 1% (v/v) 2-mercaptoethanol. Gel strips were then rinsed twice with SDS–PAGE electrophoresis buffer (25 mM Tris–HCl, 192 mM glycine and 0.1% (w/v) SDS; pH 8.3), and were placed onto the wells of another gel (3DE). SDS–PAGE was performed in PROTEAN II xi Cell using a 4% stacking and a 7.5–17% separating gel. Electrophoresis was carried out at 25°C with an initial current of 70 V (during the first hour). Then, the voltage was set to 100 V for the next 12 h (overnight), and increased to 200 V until the dye front reached the bottom of the gel. Colloidal Coomassie blue staining was used for visualization.

In-gel digestion of purified myelin fraction with trypsin

The gel pieces of interest were cut into small pieces to increase surface and collected in a 0.6 ml tube. They were initially washed with 50 mM ammonium bicarbonate and then twice with 50% 50 mM ammonium bicarbonate/50% acetonitrile for 30 min with occasional vortexing. The washing solution was discarded at the end of each step. 100 microlitre of 100% acetonitrile was added to each tube to cover the gel piece followed by incubation for at least 5 min. The gel pieces were dried completely in a Speedvac Concentrator 5301 (Eppendorf, Germany). Cysteines were reduced with a 10 mM dithiothreitol solution in 0.1 M ammonium bicarbonate pH 8.6 for 60 min at 56°C. The same volume of a 55 mM solution of iodoacetamide in 0.1 M ammonium bicarbonate buffer pH 8.6 was added and incubated in darkness for 45 min at 25°C to alkylate cysteine residues. The reduction/alkylation solutions were replaced by 50 mM ammonium bicarbonate buffer for 10 min. Gel pieces were washed and dried in acetonitrile followed by Speedvac concentration.

The dried gel pieces were re-swollen with 12.5 ng/μl trypsin (Promega, WI, USA) solution buffered in 25 mM ammonium bicarbonate. They were incubated for 16 h (overnight) at 37°C. Supernatants were transferred to new 0.6 ml tubes, and gel pieces were extracted again with 50 μl of 0.5% formic acid/20% acetonitrile for 15 min in a sonication bath. This step was performed twice. Samples in extraction buffer were pooled in a 0.6 ml tube and evaporated in a Speedvac. The volume was reduced to ~10 μl and 10 μl water was added.

Protein identification with Nano-HPLC-ESI-Q-TOF mass spectrometry

LC-ESI-MS/MS analyses were carried out with the UltiMate 3000 system (Dionex Corporation, Sunnyvale, CA, USA) interfaced to the QSTAR Pulsar mass spectrometer (Applied Biosystems, Foster City, CA, USA). A nanoflow HPLC equipped with a reversed phase PepMap C-18 analytic column (75 μm × 150 mm) was used. Chromatography was performed using a mixture of two solutions, A (0.1% formic acid in water) and B (80% acetonitrile/0.85% formic acid in water), with a flow rate of 300 nl/min. First a linear gradient between 4% and 60% B was run over 45 min, then 90% B was used for 5 min and 0% B for 25 min. Peptide spectra were recorded over the mass range of *m/z* 350–1300, and MS/MS spectra were recorded under information dependent data acquisition (IDA) over the mass range of *m/z* 50–1300. One peptide spectrum was recorded followed by three MS/MS spectra on the QSTAR Pulsar instrument; the accumulation time was 1 s for peptide spectra and 2 s for MS/MS spectra. The collision energy was set automatically according to the mass and charge state of the peptides chosen for fragmentation. Doubly or triply charged peptides were chosen for MS/MS experiments due to their good fragmentation characteristics. MS/MS spectra were interpreted by the MASCOT software (mascot.dll 1.6b21; Matrix Science, London, UK) in Analyst QS 1.1 (Applied Biosystems). Searches were done by using the MASCOT 2.1 (Matrix Science, London, UK) against Swissprot 53.3 and MSDB 20051115 database for protein identification. Searching parameters were set as follows: enzyme selected as trypsin with a maximum of two missing cleavage sites, species limited to mouse, a mass tolerance of 500 ppm for peptide tolerance, 0.2 Da for MS/MS tolerance, fixed modification of carbamidomethyl (C) and variable modification of methionine oxidation and phosphorylation (Tyr, Thr and Ser).

Immunocytochemistry

The pooled OPCs harvested as outlined above were seeded at a density of 20 000 cells per well into PLL-coated eight-well chamber slides. Cells were differentiated for 48 h and subsequently fixed with 4% paraformaldehyde in PBS, permeabilized and blocked with 0.3% Triton X-100 and 10% NGS. To assess the differentiation state of OPCs the cells were incubated with O4 antibody (1:100; Millipore Corporation, Billerica, MA, USA) for 1 h in the presence of 0.1% Triton X-100 and 2% NGS, washed, and incubated for another 1 h with the appropriate fluorescent secondary antibody (Cy3-conjugated antibody 1:100; Jackson Immuno Research, Suffolk, UK) and the nuclei were stained using DAPI (Robinson and Miller, 1999; Syed *et al*., 2008). It is important to note that permeabilization of cells results in a punctate representation of the extracellular antigen O4 (Reynolds and Weiss, 1993; Weiss *et al*., 1996; Syed *et al*., 2008). Under an Olympus X51 fluorescent microscope using a triple-filter we determined the percentage of O4-positive cells in relation to >100 DAPI-stained nuclei in randomly selected eye fields for each experimental condition.

To establish the purity of our OPC cultures immunocytochemistry for A2B5 (1:100; Millipore Corporation, Billerica, MA, USA) was performed according to the same principles and the percentage of A2B5+ cells to >100 DAPI-stained nuclei in randomly selected eye fields was determined. Only cell cultures with >94% A2B5+ cells were used for our study. To assess the morphological phenotype of OPCs, A2B5+ cells were categorized according to the following criteria: stage I: mono/bipolar; stage II: multipolar, primary branched; stage III: multipolar, secondary branched; stage IV: secondary branched cells with membranous processes.

qPCR for myelin basic protein versus β-2-microglobulin

Total RNA of OPCs grown on PLL control or MPE substrates with various concentrations (0.4 μg MPE, 4 μg MPE and 40 μg MPE) was harvested after the cells were differentiated for 3 days using RNeasy Mini Kit (Quiagen, Hilden, Germany) according to the manufacturer's instruction.

First strand cDNA synthesis kit for RT–PCR (Roche Applied Science, Vienna, Austria) was used for reverse transcription of 500 ng RNA (each sample) according to the manufacturer's instructions.

q-PCR was performed using Taqman gene expression assays for myelin basic protein (MBP) (ABI, Foster City, CA, USA, Rn 00566745_M1) and β-2-microglobulin (β2-MG) (ABI, Rn 00560865). Three independent experiments were conducted and all reactions were performed in triplicate on a 7500 Fast Real-Time PCR System. Semi-quantitative mRNA expression levels were calculated with the 7500 Fast System Software (ABI, Foster City, CA).

Pharmacological inhibition of ROCK-II and PKC

To examine whether ROCK-II and PKC signal transduction is implicated in the myelin mediated differentiation block, pharmacological inhibitors were added to the culture medium immediately after cell seeding. The selective PKC-inhibitor Gö6976 specific for PKC-α and PKC-β (12-(2-cyanoethyl)-6,7,12,13-tetrahydro-13-methyl-5-oxo-5H-indolo[2,3-a]pyrrollo[3,4-c]carbazole; CAS-number: 136194-77-9) and BIM (Ro 31-8220, Bisindolylmaleimide IX; CAS-number: 125314-64-9) selectively affecting all PKC isoforms were used to block PKC-signalling. To inhibit ROCK-II, an orally available drug currently evaluated for the treatment of vascular disease named Fasudil

(HA-1077 dihydrochloride; 1-(5-Isoquinolinesulfonyl)-1H-hexahydro-1,4-diazepine 2 HCl; CAS-number: 103745-39-7) was used with the potential of interfering with Rho kinase, PRK2, MSK1, PKA, PKG, S6K1, MAPKAP-K1b, MLCK and CaMKII signalling. Gö6976 and BIM were solubilized in DMSO. OPCs plated on different substrates were differentiated for 48 h and subsequently fixed for immunocytochemistry. To quantitate differentiation, the ratio of O4 positive cells and the number of Hoechst-positive nuclei was determined by cell counts using an Olympus IX 51 fluorescence microscope. A minimum of 200 cells were counted for each experiment and a minimum of three independent experiments were conducted.

siRNA-based downregulation of RhoA and PKC-α

Ten days after plating mixed glial cultures were transfected with siRNA for PKC-α, RhoA, negative control siRNA and Cy^{TM3} labelled negative control (Applied Biosystems) using Lipofectamine 2000 (Invitrogen, Paisley, UK) at a concentration of 100 nM according to the manufacturer's protocol. Twenty-four hours later OPCs were harvested as outlined above. To determine the knock-down efficiency of the targeted genes Western blot analyses were performed for RhoA (Millipore Corporation) or PKC-α (Cell Signalling, Danvers, MA, USA). OPC differentiation was assessed as outlined above 48 h after plating cells onto the experimental substrates; at least three independent experiments were conducted for each condition.

TUNEL assay

Fragmented DNA was detected by incorporation of biotinylated nucleotides at the 3′-OH DNA ends using terminal deoxynucleotidyl transferase recombinant (rTdT) enzyme according to the manufacturer's instruction (Promega, Madison, WI, USA). Stained cells were visualized by light microscopy and the percentage of apoptotic nuclei was determined.

Western blot analysis

OPCs differentiated for 24 h and 9 days on PLL were lysed in a buffer containing 10 mM Tris, pH 7.4, 100 mM NaCl, 1 mM EDTA, 1 mM EGTA, 1 mM NaF, 20 mM $Na_4P_2O_7$, 2 mM Na_3VO_4, 0.1% SDS, 0.5% Sodium Deoxcholate, 1%Triton-X100, 10% Glycerol, 1 mM PMSF, 60 μg/ml Aprotinin, 10 μg/ml Leupeptin, 1 μg/ml Pepstatin. After high speed centrifugation, protein concentration was measured using BCA^{TM} protein assay (Pierce) and 15 μg were loaded on SDS–PAGE for separation. Western blot was conducted using a Multiphor II Electrophoresis System (GE Healthcare UK Ltd) at 200 mA for 1.30 h. After blocking with 5% BSA in TBS-T (0.1% Triton X 100 in TBS) for 1 h at room temperature the blots were incubated with antibodies against ROCK II/ROKα (BD Biosciences, San Jose, CA, USA), RhoA (Millipore Corporation) or PKC-α (Cell Signalling) antibodies over night (4°C). Following incubation with horseradish-peroxidase conjugated secondary antibody (GE Healthcare UK Ltd) for 1 h the immunoreactive bands were detected by ECL^{TM} chemiluminescence (GE Healthcare UK Ltd) reagent on a film.

To confirm the presence of proteins identified by MS analysis in the purified inhibitory fractions, 10 μg of protein was separated using 12% Novex gel (Invitrogen). MPE was used as positive control and protein extracts of liver membrane preparation as negative control. Following SDS–PAGE, the protein was then transferred to PVDF membrane using an Xcell II Blot Module (Invitrogen). After blocking with 5% BSA in TBS-T (0.1% Triton X 100 in TBS) for 1 h at room temperature it was probed overnight at 4°C with the following antibodies: myelin-associated glycoprotein (MAG) (Millipore Corporation), PLP (kindly provided by Lees MB), MBP (DAKO). Following a wash step the membranes were incubated with the appropriate horseradish-peroxidase conjugated secondary antibody (GE Healthcare UK Ltd) for 1 h. The immunoreactive bands were detected by ECL^{TM} chemiluminescence (GE Healthcare UK Ltd) reagent on a film.

Evaluation of Fyn activation

Cells were washed twice with ice cold PBS before being lysed in 10 mM Tris, 100 mM NaCl, 1 mM EDTA, 1 mM EGTA, 1 mM NaF, 2 mM Na_3VO_4, 0.1% Triton, 10% Glycerol, 1 mM PMSF, 0.5% Na-Deoxycholate, 20 mM $Na_4P_2O_7$ and protease inhibitor (Roche). Cell lysates were centrifuged (1 h, 3200 rpm, 4°C) and the protein concentration was estimated by BCA^{TM} assay (Pierce). The lysates were pre-cleared with A/G Plus Agarose beads (Santa Cruz, CA, USA) for 30 min at 4°C and incubated with total Fyn antibody (Santa Cruz) for 2 h in a rotary mixer following addition of A/G Plus Agarose beads for overnight incubation. Before performing SDS–PAGE and Western blot the immune complexes were washed extensively with NP-40 buffer and PBS. The precipitates were re-suspended in sample buffer, heated to 95°C for 5 min, and subjected to SDS–PAGE. Proteins were transferred to a PVDF membrane, blocked with bovine serum albumin and incubated with Y-418-phospho-Src (Biosource) antibody. Finally a horseradish-peroxidase conjugated secondary antibody was added and detected by ECL^{TM} chemiluminescence (GE Healthcare UK Ltd) reagent on film. The optical density of the bands was estimated with NIH-Image J (free download at http://rsb.info.nih.gov/ij/) on digitized images.

RhoA GTPase activity assay

For the detection of active RhoA, OPCs were lysed (125 mM HEPES, pH 7.5, 750 mM NaCl, 5% Igepal CA-630, 50 mM $MgCl_2$, 5 mM EDTA, 10% Glycerol, 25 mM NaF, 1 mM Na_3VO_4) according to the manufacturer's instructions (Millipore Corporation) and active GTP-Rho was precipitated by the use of beads specific for the GST-binding domain (RBD) of rhotekin. After removing cell debris the lysates were incubated with Rho Assay Reagent Slurry, which specifically binds Rho-GTP and not Rho-GDP (30 min, 4°C). Beads were then washed with Mg^{2+} lysis/wash buffer and bound material was eluted with 25 μl 2× Laemmli sample buffer, boiled for 5 min, resolved by SDS–PAGE and immunoblotted using mouse anti-RhoA antibody (3 μg/ml). Peroxidase-conjugated anti-mouse IgGs (GE Healthcare UK Ltd) were used as secondary antibodies. Immunoreactive proteins were visualized using ECL^{TM} detection system (GE Healthcare UK Ltd). Densitometric analysis was performed using NIH-Image J software.

Statistical analysis

For all studies at least three independent experiments (*n* as detailed in results) were conducted and statistically assessed using Graph Pad Prism software (Graph Pad, San Diego, CA). To test the concentration dependent inhibition of OPC differentiation on MPE and the effect of various concentrations of pharmacological inhibitors one way ANOVA followed by Dunett's multiple comparison test was used. ROD values from Western blot following immunoprecipitation or pull-down assay were compared with Student-*t*-test.

Results

Soluble myelin molecules inhibit the differentiation of OPCs

To establish an *in vitro* assay for assessing the effects of myelin on OPC differentiation we adapted an approach previously reported by Robinson and Miller and plated neonatal OPCs on myelin substrates produced by incubation of myelin preparations on poly-L-lysine covered culture dishes (Robinson and Miller, 1999). The differentiation of oligodendrocyte lineage cells (OLCs) *in vitro* is characterized by distinct morphological and immunological features. Antibodies against O4 identify late OPCs by reacting with a sulphated glycolipid antigen named POA (Proligodendrocyte Antigen), while the same antibody also recognizes terminally differentiated OLCs by reacting with sulphated galactosylcerebroside (Bansal *et al*., 1989). The differentiation block mediated by presence of myelin is manifested as a reduction in O4-expression by OPCs (Robinson and Miller, 1999). In a previous study we showed that MPEs prepared with *n*-octyl-glycoside induce a concentration-dependent inhibition of differentiation in OPCs cultured in differentiation medium for 48 h similar to that observed with crude myelin membrane preparations (Syed *et al*., 2008). The inhibition of OPC differentiation is not only reflected by a reduction of O4 expression but also by a corresponding downregulation of mRNA expression for MBP, a late marker of mature oligodendrocytes, as assessed by qPCR (Fig. 1; $n=3$). The presence of myelin was associated with a reduction in the complexity of OPC processes resulting in an increase of early OPC phenotypes with bipolar (stage I) morphology or primary branches (stage II) and a consecutive reduction of OPCs with secondary branched or membranous processes (stage III/IV) (Fig. 6) (one-way ANOVA $P<0.0001$). We also confirmed previous data (Robinson and Miller, 1999) demonstrating that no changes occurred in the rate of cell proliferation as assessed by BrdU staining (no BrdU-positive cells were detected in the experimental groups) or apoptosis assessed by TUNEL assay, indicating that differences in the proportion of O4-positive cells reflect changes of cell differentiation and that these were not caused by an increase of OPC proliferation or differences in the rate of apoptosis (Supplementary Fig. 1).

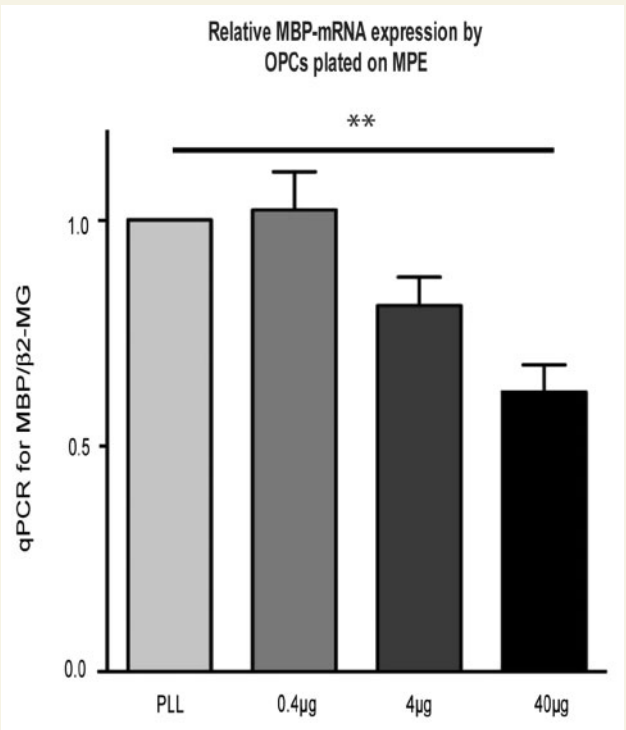

Fig. 1 OPCs plated on MPEs (protein/cm^2) display a concentration dependent down-regulation of relative MBP mRNA expression as assessed by qPCR after 3d culture in differentiation medium (for this and subsequent figures: MPE: myelin protein extract; error bars: SEM).

Purification of inhibitory myelin fractions and proteomic analysis

The myelin proteins responsible for the inhibition of OPC differentiation are unknown. The most prominent myelin associated inhibitors (MAI) NogoA, MAG and Omgp do not affect OPC differentiation (Syed *et al*., 2008). To identify potential candidates we developed a column-chromatography fractionation protocol. In the first step MPE was submitted to a CM-column, and the resulting fractions tested by plating OPCs on the eluates. The fraction carrying inhibitory activity was then submitted to a second purification step using an ion exchange column (HighQ). The eluates obtained were tested in the same manner and the final inhibitory fraction was used for proteomic analysis.

To identify the protein species contained in the inhibitory fraction we employed a 3D gel-based separation protocol (BN-SDS-SDS) specifically tailored for identification of membrane-bound proteins (Kang *et al*., 2008). The protein spots on the 12 resulting gels were picked, digested and analysed on a nano-HPLC-ESI-Q-TOF mass spectrometer. The proteins identified are presented in Table 1 according to their annotation to the spots picked (Supplementary Fig. 2A–F). Of the 137 proteins detected, 18 were previously identified in proteomic analyses of myelin membrane fractions (Taylor and Pfeiffer, 2003; Taylor *et al*., 2004; Vanrobaeys *et al*., 2005; Werner *et al*., 2007). To confirm the presence of selected protein species we conducted Western blots on fractions generated as outlined above (Supplementary Fig. 3). These data provide a list of potential candidates that may be responsible for the inhibitory effect on OPC differentiation and illustrate the complexity of the myelin proteome, which becomes specifically apparent when highly abundant protein species are removed by column-chromatography based separation techniques.

Myelin impairs activation of the Src family tyrosine kinase Fyn-1

To investigate the basis of the myelin mediated inhibition of OPC differentiation we examined the activation of Src family tyrosine kinase Fyn-1. Several lines of evidence implicate an important role for Fyn-1 in the formation of myelin sheaths: first, the myelin content found in brains of fyn-deficient mice is reduced, and

Table 1 Identified protein list from BN/SDS/SDS–PAGE (3DE) from purified myelin protein fraction

Protein Name	Swiss-Prot ID	NCBI Acc. No[a]	Theoretical molecular weight	No. of TMD[b]	Total ion-score	No. of matched peptides (MS/MS)	Sequence coverage (%)	Spot No.
Known myelin proteins								
Myelin-associated glycoprotein precursor	P07722	gil126685	69353	1	294	8	21	18
Myelin basic protein S	P02688	gil17378709	21546	0	36	1	5	131
Myelin-oligodendrocyte glycoprotein precursor	Q63345	gil2497314	27882	2	112	3	13	77
Myelin proteolipid protein	P60203	gil41019153	30077	4	124	3	18	3
Membrane proteins								
Abhydrolase domain-containing protein 6	Q5XI64	gil81883706	38312	1	155	4	13	89
Acyl-CoA-binding domain-containing protein 5	A0FKI7	gil123797828	56782	1	59	1	4	58
Basigin precursor	P26453	gil51704207	42436	1	89	2	5	117
Brain acid soluble protein 1	Q05175	gil730110	21790	0	321	10	41	17
CD9 antigen	P40241	gil729088	25215	4	239	7	32	2
CD63 antigen	P28648	gil113331	25699	4	79	2	11	101
CD81 antigen	Q62745	gil11131474	25889	4	211	5	16	4
CD82 antigen	O70352	gil9296930	29487	4	45	2	10	21
CD151 antigen	Q9QZA6	gil11131479	28355	4	160	4	20	51
CD166 antigen precursor	O35112	gil47605356	21635	1	194	6	29	74
Cell adhesion molecule 2 precursor	Q1WIM2	gil150438865	47528	1	194	4	11	53
Cell adhesion molecule 4 precursor	Q1WIM1	gil123778954	42781	1	193	6	15	28
Cell cycle exit and neuronal differentiation protein 1	Q5FVI4	gil81882797	15043	1	88	3	23	44
Choline transporter-like protein 1	Q8VII6	gil73918925	73092	10	61	3	4	27
Clathrin coat assembly protein AP180	Q05140	gil2492686	93519	0	96	3	3	92
Claudin-11	Q99P82	gil20532024	22046	4	189	6	37	45
Disks large-associated protein 2	P97837	gil71153508	118978	0	164	6	8	34
DnaJ homolog subfamily C member 5	P60905	gil46397406	22101	0	42	2	11	50
Ectonucleotide pyrophosphatase/phosphodiesterase family member 5 precursor	P84039	gil108862048	54290	1	164	5	12	71
Embigin precursor	O88775	gil61223483	37005	1	176	5	23	72
Erythropoietin receptor precursor	Q07303	gil729431	55500	1	88	4	6	94
FXYD domain-containing ion transport regulator 6 precursor	Q91XV6	gil20138106	10388	1	229	7	26	63
FXYD domain-containing ion transport regulator 7	P59649	gil30315809	8487	1	38	1	19	5
Golgin subfamily A member 2	Q62839	gil6226622	111428	0	106	3	4	14
Junctional adhesion molecule C precursor	Q68FQ2	gil83286894	34783	1	168	5	16	38
Leukocyte surface antigen CD47 precursor	P97829	gil76364105	32995	5	69	3	14	33
Limbic system-associated membrane protein precursor	Q62813	gil2497324	37324	0	114	2	7	26
Lysosome-associated membrane glycoprotein 1 precursor	P14562	gil126378	43969	1	225	5	11	16
Lysosome-associated membrane glycoprotein 2 precursor	P17046	gil126382	45591	1	203	6	17	136
Lysosome membrane protein 2	P27615	gil126291	54091	2	268	12	33	22
Major prion protein precursor	P13852	gil2507236	27804	0	33	1	7	49
Membrane transport protein XK	Q5GH61	gil77417634	51050	10	133	4	10	23
Metabotropic glutamate receptor 4 precursor	P31423	gil400255	101819	7	39	2	1	121
Myosin-9	Q62812	gil13431671	226338	0	108	4	2	102
Neural cell adhesion molecule 1, 140 kDa isoform precursor	P13596	gil127859	94658	1	203	5	6	115

(continued)

Table 1. Continued

Protein Name	Swiss-Prot ID	NCBI Acc. No[a]	Theoretical molecular weight	No. of TMD[b]	Total ion-score	No. of matched peptides (MS/MS)	Sequence coverage (%)	Spot No.
Neurofilament medium polypeptide	P12839	gil128150	95791	0	110	4	6	128
Neuromodulin	P07936	gil128102	23603	0	116	3	14	110
Neuroplastin precursor	P97546	gil81870588	31292	1	278	7	36	19
Neurotrimin precursor	Q62718	gil2497325	37998	0	44	2	7	39
Nicastrin precursor	Q8CGU6	gil37081094	78400	1	332	12	32	15
Neuritin precursor	O08957	gil81882120	15289	0	103	3	10	66
Nuclear envelope pore membrane protein POM 121	P52591	gil1709213	120785	1	226	5	4	80
Opioid-binding protein/cell adhesion molecule precursor	P32736	gil1352640	38068	0	138	3	11	25
Phosphatidylethanolamine-binding protein 1	P31044	gil400734	20801	0	154	5	21	62
Phospholemman precursor	O08589	gil22654268	10365	1	100	3	19	60
Prostaglandin-H2 D-isomerase precursor	P22057	gil1346697	21301	0	201	4	16	137
Protocadherin Fat 2 precursor	O88277	gil22095688	480654	1	119	3	6	57
Sodium channel protein type 9 subunit alpha	O08562	gil55976160	226039	24	144	5	2	83
Sodium channel subunit beta-2 precursor	P54900	gil1705870	24145	1	121	4	19	36
Sodium/potassium-transporting ATPase subunit beta-1	P07340	gil114395	35202	1	88	3	7	56
Synaptosomal-associated protein 23	O70377	gil41017815	23235	0	79	2	9	65
Synaptosomal-associated protein 25	P60881	gil46397720	23315	0	114	3	8	67
Syntaxin-1B	P61265	gil47117736	33245	1	188	6	17	64
Tetraspanin-2	Q9JJW1	gil23396887	24190	4	63	2	8	29
Thioredoxin domain-containing protein C5orf14 homolog	Q5BJT4	gil81882519	37928	1	205	5	8	107
Tyrosine-protein phosphatase non-receptor type substrate 1 precursor	P97710	gil29427383	55691	1	105	4	10	122
Thy-1 membrane glycoprotein precursor	P01830	gil135832	18172	0	99	3	11	130
Voltage-dependent anion-selective channel protein 2	P81155	gil46397780	31746	0	133	5	14	37
2′,3′-cyclic-nucleotide 3′-phosphodiesterase	P13233	gil51338709	47268	0	319	6	13	7
Cytoplasmic proteins								
Amphiphysin	O08838	gil14916529	74878	0	118	3	5	114
Branched-chain-amino-acid aminotransferase, cytosolic	P54690	gil1705438	46046	0	226	7	24	98
Calmodulin	P62161	gil49037408	16838	0	125	3	16	111
Coiled-coil domain-containing protein 93	Q5BJT7	gil81882521	72636	0	152	4	6	104
COP9 signalosome complex subunit 1	P97834	gil2494624	53428	0	108	4	9	24
ERC protein 2	Q8K3M6	gil51701368	110618	0	98	2	3	42
FKBP12-rapamycin complex-associated protein	P42346	gil1169736	288794	0	68	2	1	87
Glial fibrillary acidic protein	P47819	gil115311597	49957	0	113	3	10	31
Glutathione transferase omega-1	Q9Z339	gil12585231	27669	0	113	3	9	106
Heat shock cognate 71 kDa protein	P63018	gil51702273	70871	0	271	5	6	135
Huntingtin	P51111	gil1708162	343762	0	101	3	1	91
Hypoxanthine-guanine phosphoribosyltransferase	P27605	gil123501	24477	0	32	1	4	124
Junction plakoglobin	Q6P0K8	gil81885083	81801	0	105	4	5	41
LAMA-like protein 2 precursor	Q4QQW8	gil146324959	65456	0	201	5	9	90
Myc box-dependent-interacting protein 1	O08839	gil14916534	64533	0	229	8	12	113
NAD-dependent deacetylase sirtuin-2	Q5RJQ4	gil81883338	39319	0	91	2	5	109

Neurocalcin-delta	Q5PQN0	gil81909955	22245	0	126	4	20	61
Neuron-specific calcium-binding protein hippocalcin	P84076	gil51317364	22427	0	98	4	23	59
glycosyltransferase GLT28D1	Q5I0K7	gil81883003	18329	0	62	2	7	69
Phenylalanyl-tRNA synthetase alpha chain	Q505J8	gil81887353	57720	0	88	2	5	118
Phosphatidylinositol 4,5-bisphosphate 5-phosphatase A	Q9JMC1	gil30315961	107208	0	97	4	3	88
Protein kinase C and casein kinase substrate in neurons protein 1	Q9Z0W5	gil22256946	50449	0	114	5	14	116
Protein S100-A3	P62819	gil51338664	11747	0	52	1	14	12
Protein S100-A6	P05964	gil46397773	10035	0	89	2	28	11
Protein S100-B	P04631	gil134139	10744	0	98	3	18	68
Superoxide dismutase [Cu-Zn]	P07632	gil134625	15912	0	106	2	13	55
Thioredoxin	P11232	gil135776	11673	0	135	4	24	1
Tropomyosin alpha-1 chain	P04692	gil92090646	32681	0	88	2	6	76
Tropomyosin alpha-3 chain	Q63610	gil148840439	29007	0	76	2	7	75
Ubiquitin carboxyl-terminal hydrolase 19	Q6J1Y9	gil81863791	150302	0	119	6	3	99
UDP-glucose:glycoprotein glucosyltransferase 1 precursor	Q9JLA3	gil68052986	174049	0	157	3	2	81
Visinin-like protein 1	P62762	gil51338688	22142	0	213	6	31	78
14-3-3 protein zeta/delta	P63102	gil52000883	27771	0	228	7	28	54
Nuclear proteins								
Calpain-5	Q8R4C0	gil28376969	73065	0	155	5	10	96
Cell division cycle 5-related protein	O08837	gil73619939	92218	0	33	3	3	79
DNA repair protein RAD50	Q9JIL8	gil60392975	153784	0	223	5	3	125
Histone H2B type 1	Q00715	gil399856	13990	0	123	3	21	8
Histone H2B type 1-A	Q00729	gil399855	14225	0	109	2	26	9
Histone H3.1	Q6LED0	gil81863898	15404	0	49	1	8	13
Histone H4	P62804	gil51317315	11367	0	102	3	34	10
La-related protein 7	Q5XI01	gil134034153	64949	0	32	3	10	129
RING finger protein 181	Q6AXU4	gil81891326	19288	0	34	2	9	119
Small ubiquitin-related modifier 2 precursor	P61959	gil48429128	10871	0	76	3	13	108
Structural maintenance of chromosomes protein 3	P97690	gil29336525	138448	0	149	4	3	82
UV excision repair protein RAD23 homolog B	Q4KMA2	gil123789085	43497	0	133	4	7	112
Vimentin	P31000	gil401365	53733	0	251	6	14	103
Zinc finger CCCH type antiviral protein 1	Q8K3Y6	gil47117346	86771	0	100	4	7	84
Secreted proteins								
Alpha-1-antiproteinase precursor	P17475	gil112889	46136	0	164	5	19	97
Apolipoprotein D precursor	P23593	gil114035	21635	0	162	5	25	47
C-reactive protein precursor	P48199	gil1345834	25468	0	65	3	17	20
Serine protease inhibitor A3K precursor	P05545	gil266407	46562	0	211	6	16	85
Serine protease inhibitor A3L precursor	P05544	gil2507387	46277	0	206	5	16	86
Sulfated glycoprotein 1 precursor	P10960	gil134219	61124	0	264	5	10	6
Transthyretin precursor	P02767	gil136467	15720	0	76	2	10	134
Extracellular proteins								
Annexin A8	Q4FZU6	gil123792388	36706	0	151	4	15	52
Hemoglobin subunit alpha-1/2	P01946	gil122477	15329	0	255	7	39	48
Hemoglobin subunit beta-1	P02091	gil122514	16083	0	245	8	36	46
Lysosomal proteins								

(continued)

Table 1. Continued

Protein Name	Swiss-Prot ID	NCBI Acc. No[a]	Theoretical molecular weight	No. of TMD[b]	Total ion-score	No. of matched peptides (MS/MS)	Sequence coverage (%)	Spot No.
Cathepsin D precursor	P24268	gi|115720	44681	0	126	5	16	32
Deoxyribonuclease-2-beta precursor	Q9QZK9	gi|46395574	40472	0	83	3	7	100
Dipeptidyl-peptidase 2 precursor	Q9EPB1	gi|13626317	55114	0	83	3	6	70
N-acetylgalactosamine-6-sulfatase precursor	Q32KJ6	gi|123779981	58302	0	94	3	6	93
Palmitoyl-protein thioesterase 1 precursor	P45479	gi|1172592	34455	0	154	3	8	35
Prenylcysteine oxidase precursor	Q99ML5	gi|62286984	56288	0	164	3	9	123
Mitochondrial protein								
Apoptosis-inducing factor 1, mitochondrial precursor	Q9JM53	gi|13431757	66723	0	35	1	2	120
Unknown protein								
Putative uncharacterized protein ENST00000281581 homolog	Q5PQJ9	gi|117940141	96777	0	185	4	3	126

a NCBI accession number (Acc. No.) is referred in website (http://www.ncbi.nlm.nih.gov/sites/entrez). b Theoretical number of transmembrane domain (TMD) was calculated in website (http://www.expasy.org).

second, Fyn-1 can be co-immuno-precipitated from brain lysates with antibodies to MAG (Umemori *et al*., 1994). More recent data suggest that activation of Fyn-1 is one of the earliest events triggered in differentiating OPCs and that Fyn-1 tyrosine kinase regulates process extension and myelin sheath formation (Osterhout *et al*., 1999; Colognato *et al*., 2004).

Protein extracts from OPCs plated on MPE cultured in differentiation medium for 24 h were compared with protein extracts from OPCs plated on control substrates under the same conditions by immuno-precipitation with anti-Fyn-1 and immunoblotting with anti-Src Y-418, to detect phosphorylation at the activation site of Fyn-1. The results demonstrated a clear impairment of Fyn-1 activation in cells plated on MPE ($n = 4$; t-test $P = 0.0003$; Fig. 2A and B). In OPCs plated on control substrate phosphorylation of Fyn-1 increased over time as previously reported (Osterhout *et al*., 1999).

Myelin molecules mediate inhibitory signals via activation of RhoA

Fyn-1 kinase regulates the activity of the small GTPase RhoA (Colognato *et al*., 2004), which, along with other Rho GTPase subfamily members is an important regulator of oligodendrocyte morphology (Mi *et al*., 2005; Thurnherr *et al*., 2006). Overexpression of dominant-negative RhoA causes hyperextension of oligodendrocyte processes (Wolf *et al*., 2001) while a reduction of active RhoA-GTP is necessary for successful oligodendrocyte differentiation (Liang *et al*., 2004). To assess activation of RhoA in OPCs cultured on MPE and control substrates for 24 h in differentiation medium we performed a RhoA-GTP-pull down assay followed by Western blot for RhoA. Our data show that the presence of myelin inhibitors induces an increase of GTP bound RhoA ($n = 3$; t-test: $P = 0.0113$; Fig. 2C and D).

To assess the functional role of RhoA in mediating inhibitory effects of MAI to OPC differentiation we transfected OPCs with siRNA specifically directed against RhoA. Cells were transfected with high efficiency (>95%). This induced a marked down-regulation of the expression of RhoA as assessed by Western blot. The reduction of RhoA powerfully triggered OPC differentiation in the presence of MPE (Fig. 5; $n = 3$; mean increase = 233%; ANOVA: $P < 0.0001$, Dunnett's post-test MPE versus siRNA: $P < 0.0001$) confirming the importance of RhoA in mediating the inhibitory effects as well as indicating that these can be beneficially modulated by inhibiting RhoA signalling in OPCs.

Inhibition of ROCK-II induces differentiation of OPCs in the presence of myelin

Rho kinases (ROCK) are important effector proteins of RhoA and phosphorylate a number of downstream molecules that regulate actin filaments (Riento and Ridley, 2003). Since ROCK-II is the isoform predominantly expressed in the CNS, we hypothesized its participation in transducing myelin derived inhibitory signals in OPCs. We first confirmed ROCK-II expression in OPCs by Western blot analysis and then examined its functional role

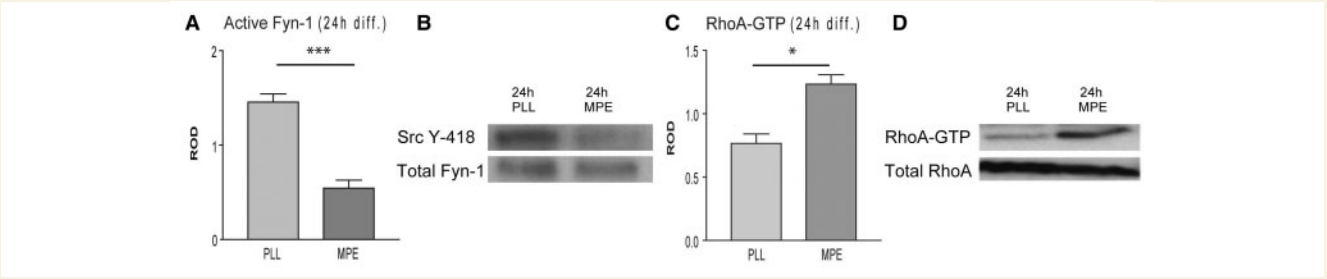

Fig. 2 (**A**) Myelin inhibitors impair Fyn-1/Y-418 phosphorylation in OPCs, (**B**) immunoblot following anti-Fyn-1-immunoprecipitation and loading control. (**C**) Myelin inhibitors also induce activation of RhoA. (**D**) Autoradiograph of Rho assay (MPE: 40 μg/cm^2; PLL: poly-L-lysine; incubation in differentiation medium for 24 h).

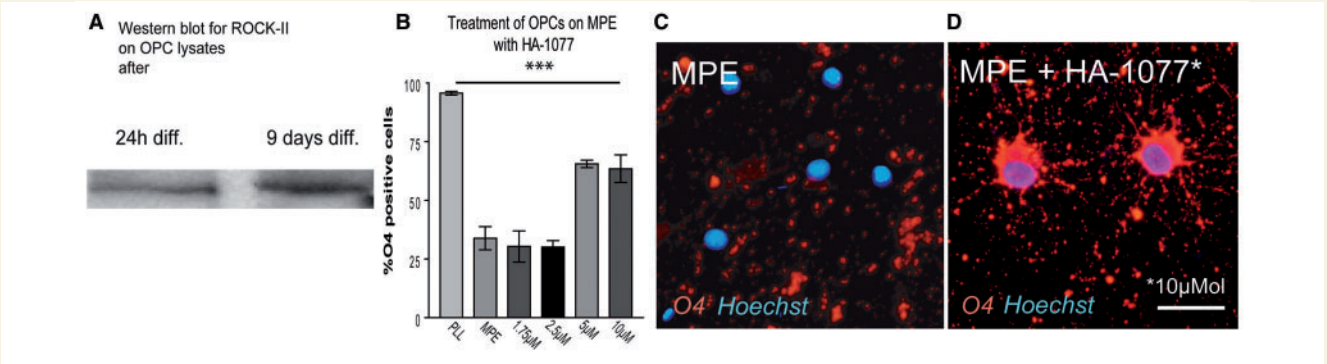

Fig. 3 (**A**) Immunoblot of OPC lysates demonstrates that differentiating OPCs express ROCK-II. (**B**) Inhibition of ROCK-II by culturing OPCs on MPE with Fasudil (HA-1077) results in a more than 160% increase of differentiating cells after 48 h culture in differentiation medium. (**C**) Whereas OPCs on MPE down-regulate O4 immunoreactivity. (**D**) O4 expression is largely restored by treatment with HA-1077 (scale bar = 30 μM).

by plating OPCs on MPE and adding different concentrations of the ROKα/ROCK II-inhibitor HA-1077 (Fasudil) to the differentiation medium (Fig. 3). Treatment with HA-1077 for 48 h resulted in a dramatic increase in the number of differentiating OPCs ($n = 4$; mean increase at 5 μM = 174%; ANOVA: $P < 0.0001$, Dunnett's post tests MPE versus 5 and 10 μM: $P < 0.001$). To exclude changes in cell survival we conducted TUNEL assays which showed no significant differences between OPCs plated on PLL and cells plated on MPE treated with HA-1077 (Supplementary Fig. 1).

Thus, we conclude that RhoA-ROCK signalling plays an important role in mediating myelin derived inhibitory effects in differentiating OPCs that can be beneficially modulated by the use of pharmacological inhibitors and siRNA-mediated gene silencing.

Myelin inhibitors retain Myristoylated, alanine-rich C-kinase substrate within the cytosolic compartment

PKC has also been implicated in OPC differentiation since PKC activation mimicked by the phorbol ester PMA inhibits OPC differentiation (Baron *et al*., 1998) while at late stages of OPC differentiation, PKC may also facilitate process extension and expression of myelin proteins (Althaus *et al*., 1991; Yong *et al*., 1991; Asotra and Macklin, 1993; Stariha and Kim, 2001). Myristoylated, alanine-rich C-kinase substrate (MARCKS) is a substrate of PKC that has been used as an indirect marker for PKC activation in OPCs (Baron *et al*., 1999). Inhibitory PKC mediated signalling is associated with phosphorylation and membrane-to-cytosol translocation of MARCKS (Baron *et al*., 1999) and may cause disorganization of the cytoskeleton and redistribution of actin filaments (Baron *et al*., 1998, 1999). MARCKS has been implicated in several cellular processes such as secretion, phagocytosis, cell motility, membrane traffic, growth suppression and regulation of the cell cycle as well as OPC differentiation (Baron *et al*., 1998, 1999; Arbuzova *et al*., 2002). Phosphorylated MARCKS is translocated from the plasma membrane to the cytosol (Wang *et al*., 1989; Thelen *et al*., 1991; Byers *et al*., 1993; Allen and Aderem, 1995). To detect changes in the intracellular distribution of MARCKS OPCs plated on MPE and control-PLL stained for A2B5 and MARCKS were compared using a laser scanning microscope (Fig. 4A–F). In differentiating OPCs MARCKS was distributed to the cell membrane whereas in OPCs in which differentiation was inhibited by the presence of MPE a clear cytosolic presence of MARCKS was detected supporting the notion that PKC is activated by myelin and that myelin inhibitors modulate cytoskeletal dynamics by MARCKS.

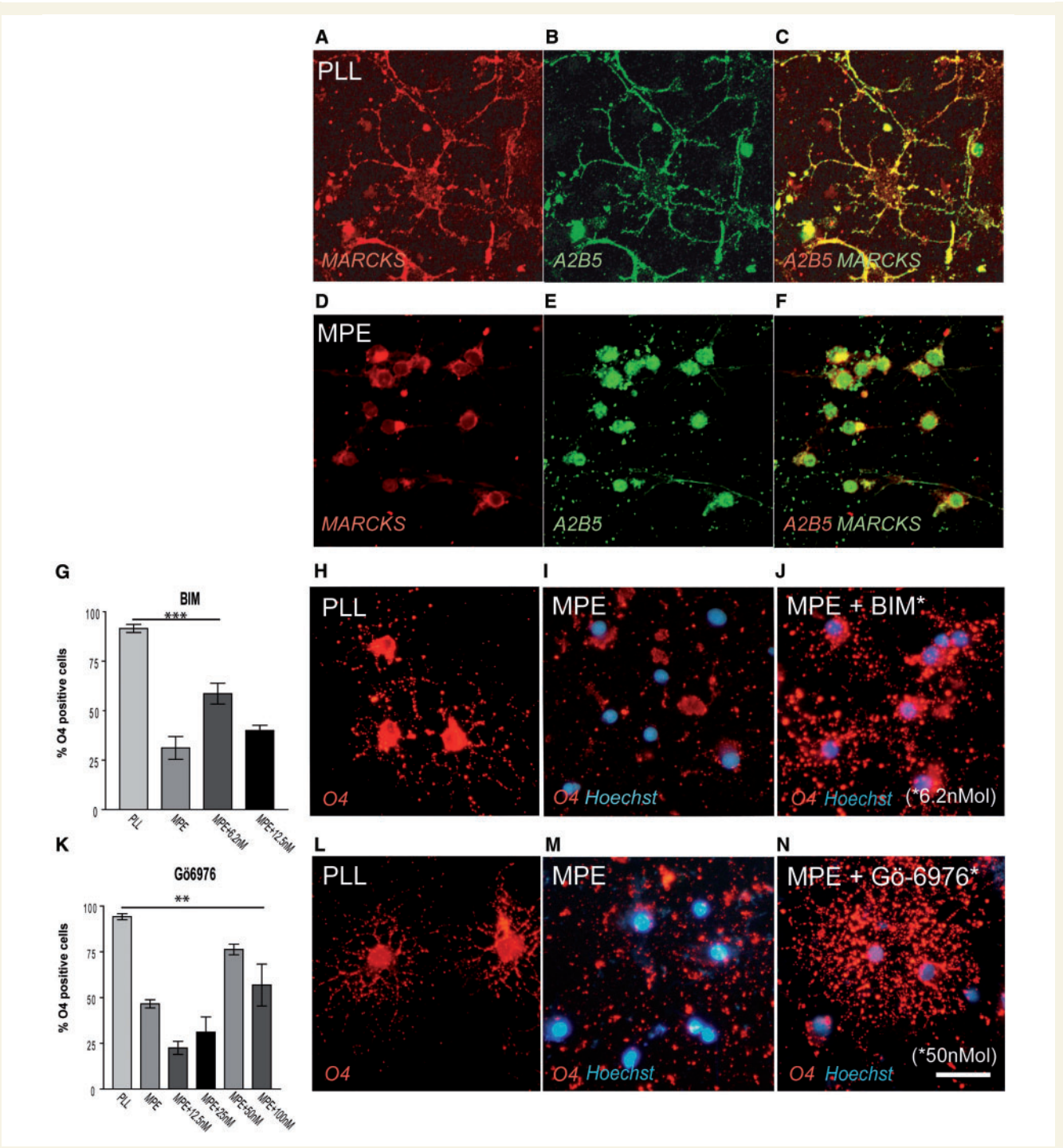

Fig. 4 (**A–F**) MARCKS is a down-stream effector of PKC. While in control cells MARCKS expression is associated with the cell membrane, myelin inhibitors lead to a cytoplasmatic MARCKS presence. (**G–N**) Inhibition of PKC signaling in OPCs on MPE with BIM (**G–J**; max. mean increase 169%) or Gö6976 (**K–N**; max. mean increase 269%) strongly induces OPC differentiation after 48 h incubation in differentiation medium. (Scalebar: in **A–C**: 15.9 μm, in **D–F**: 14.6 μm in **H–J**, **L–N**: 30 μm).

PKC inhibitors promote OPC differentiation in the presence of myelin inhibitors

In order to test whether inhibition of PKC signalling is able to modulate the myelin-mediated differentiation block OPCs plated on myelin were treated with the two selective PKC inhibitors, BIM (Bisindolylmaleimide IX, Methasulfonate Salt) and Gö6976. We found that treatment with BIM ($n = 4$; mean increase at 6.25 nM = 169%; ANOVA: $P < 0.0001$, Dunnett's post tests MPE versus 6.25 nM: $P < 0.001$; 12.5 nM: $P < 0.05$) and even more so with Gö6976 ($n = 3$; mean increase at 50 nM = 267%; ANOVA: $P < 0.0001$, Dunnett's post-test MPE versus 25 nM: $P < 0.05$;

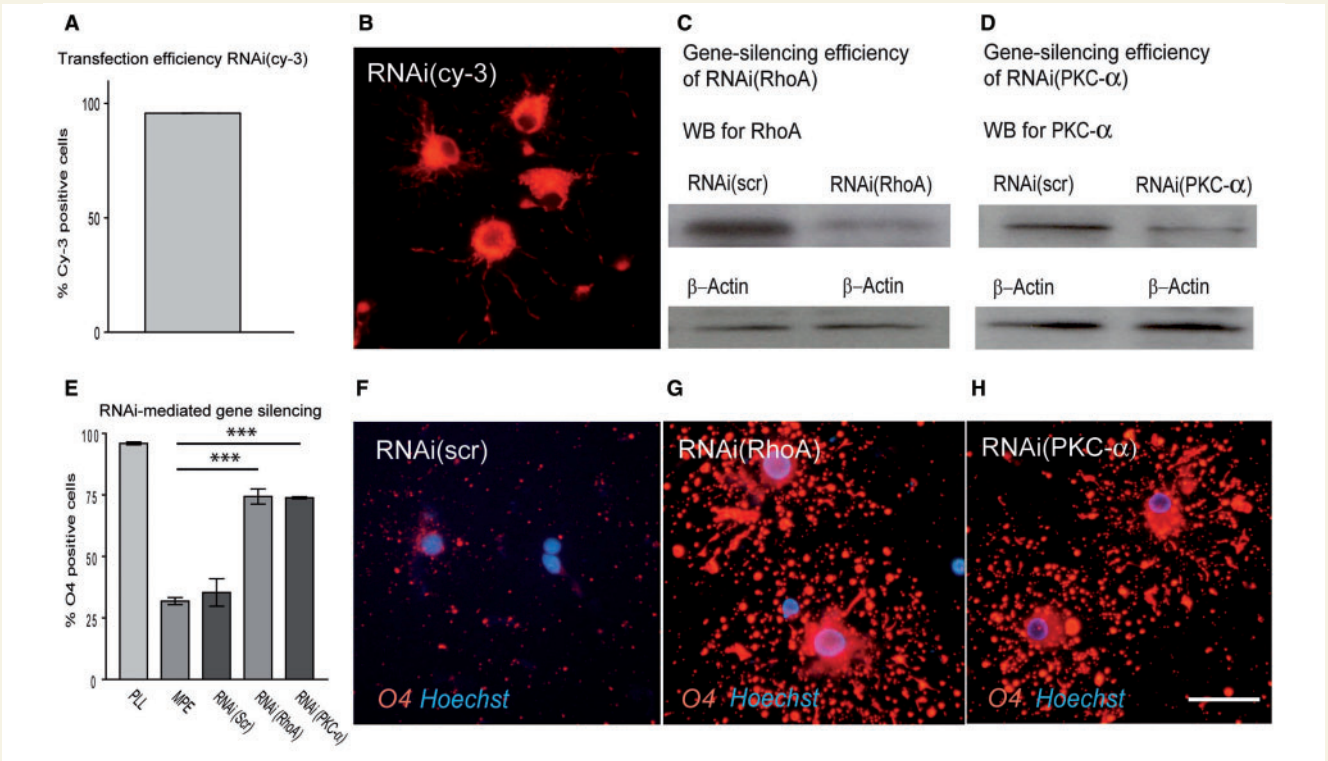

Fig. 5 (**A** and **B**) Transfection efficiency of OPCs was monitored by transfecting cells with RNAi (cy-3) and assessing the proportion of cy-3-labelled cells after 48 h in differentiation medium ($n = 3$); in all experiments >95% of the cells were cy-3 positive. Immunoblots of OPC lysates after transfection with (**C**) RNAi for RhoA as well as (**D**) RNAi for PKC-α demonstrate downregulation of RhoA or PKC-α on protein level after 48 h. (**D**) Silencing of RhoA or PKC-α results in a significant increase of O4 positive cells when cultured for 48 h on MPE. (**F**) Whereas transfection with control RNAi (RNAi(scrambled, scr)) was not able to restore O4-immunoreactivity of OPCs on MPE (**G** and **H**) gene silencing induced a strong increase in the number of differentiating cells (scalebar = 30 μM).

50 nM: $P < 0.001$) was able to stimulate OPC differentiation in the presence of myelin (Fig. 4G–N). TUNEL assays showed no differences in the rate of apoptosis between control cells and OPCs plated on myelin treated with Bim or Gö-6976 (Supplementary Fig. 1). As the use of pharmacological inhibitors entails the risk of regulating cascades other than the targeted, we used siRNA to down-regulate PKC-α expression in OPCs plated on myelin (Fig. 5). SiRNA-mediated silencing of PKC-α was successful and cells transfected displayed a marked decrease of PKC-α at protein level. The reduction of PKC-α potently induced OPC differentiation on MPE confirming the validity of the pharmacological approach ($n = 3$; mean increase = 232%; ANOVA: $P < 0.0001$, Dunnett's post test MPE versus siRNA: $P < 0.0001$) (Fig. 5).

Blocking both ROCK-II and PKC further promotes OPC differentiation

We next investigated whether ROCK-II and PKC transduce inhibitory signals via common or separate mechanisms and whether blocking both pathways at the same time could further promote OPC differentiation in the presence of myelin inhibitors. Treatment with Fasudil and Gö6976 simultaneously induced a further increase of the percentage of differentiating OPCs (Fig. 6; *t*-test: HA-1077 versus co-incubation: $P = 0.0009$; Gö6976 versus co-incubation: $P = 0.0288$). Furthermore, the treatment of OPCs on MPE with the inhibitors was able to reverse the effects of myelin on OPC morphology and resulted in the presence of more mature phenotypes (stages III and IV, Fig. 6; ANOVA of early stages (I/II) in PLL, MPE, and co-treatment $P = 0.0027$; Dunn post-test: MPE versus co-treatment $P < 0.01$). MPE may not include all inhibitory factors present in crude myelin preparations. To ensure that the beneficial treatment effects were not restricted to substrates prepared with MPE we incubated OPCs plated on crude myelin preparations with HA-1077, Gö6976, or a combination of both. This resulted in a similar induction of OPC differentiation in the presence of myelin inhibitors (data not shown). Taken together our findings suggest that the inhibitory effects of myelin molecules are mediated by at least two independent pathways. Furthermore, blocking both pathways simultaneously may provide an even more potent strategy to improve OPC differentiation in an *in vivo* setting.

Discussion

Axonal integrity is tightly coupled with myelin function as subtle changes in the molecular composition can result in mid- to long term axonal degeneration under otherwise physiological conditions (Griffiths *et al*., 1998; Garbern *et al*., 2002; Lappe-Siefke *et al*.,

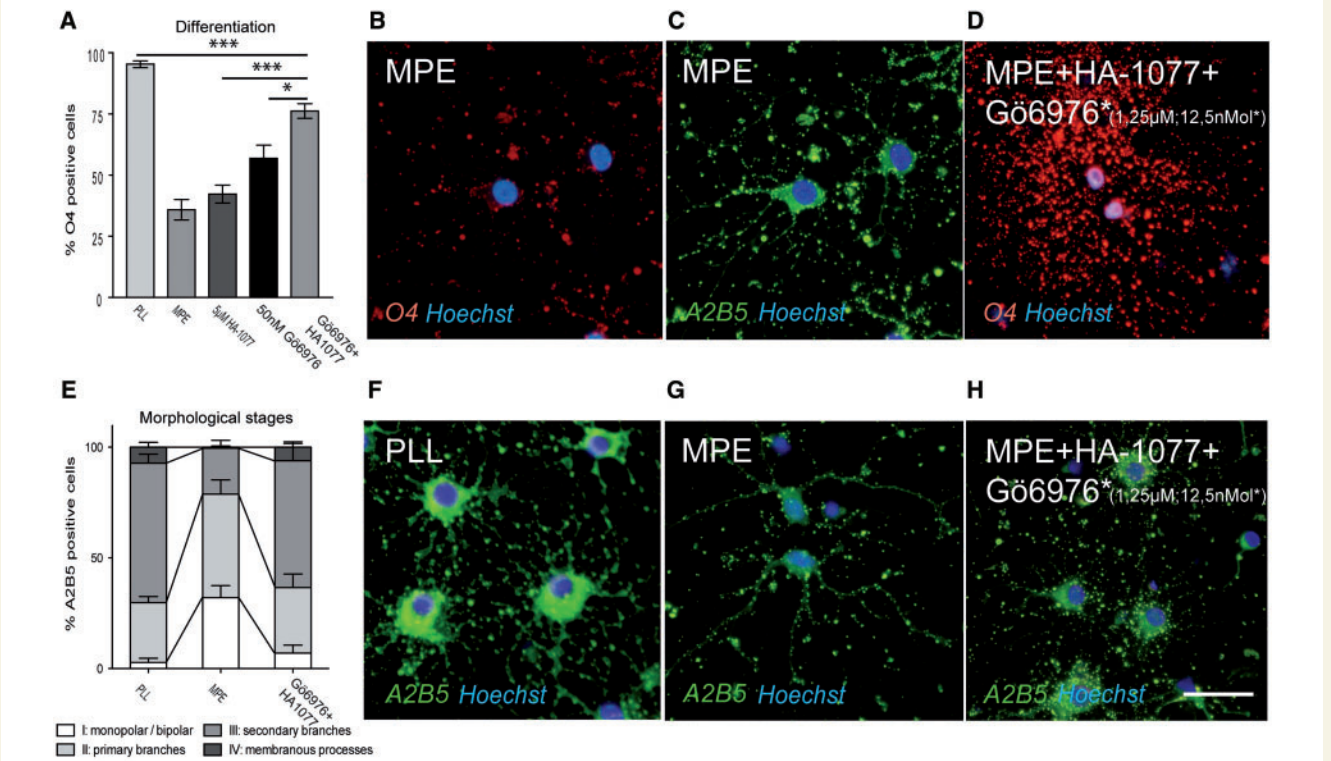

Fig. 6 (**A–C**) Blocking PKC and ROCK-II simultaneously in OPCs plated on myelin by co-incubation with HA-1077 and Gö6976 induces an additional increase in the percentage of O4-positive cells as compared to single treatment after incubation in differentiation medium for 48 h. (**B**) While MPE induces down-regulation of O4 immunoreactivity in OPCs (**C**: the same cells stained for A2B5), (**D**) O4 expression is restored after treatment with the pharmacological inhibitors. (**E–G**) The presence of MPE is associated with a reduction of the complexity of OPC processes and earlier morphological stages as compared to OPCs plated on control substrate. (**H**) Treatment with HA-1077 and Gö6976 restores the presence of more mature phenotypes (scalebar = 30 µM).

2003; Nave and Trapp, 2008). The trophic function of myelin sheaths is also very likely to be of significance for maintaining axonal integrity in both acute and chronic CNS pathology, a situation in which denuded axons may be more prone to injury or degeneration than axons bearing functionally intact myelin sheaths. Thus increasing efforts have been placed in the development of strategies by which remyelination may be enhanced therapeutically (Dubois-Dalcq *et al*., 2005). Although much is known about the biology of OPCs attempts to stimulate remyelination *in vivo* by increasing or modulating the expression proliferation or differentiation inducing factors have not been universally successful, especially when older adult animals are used in which myelin debris clearance is poor and remyelination inefficient (Shields *et al*., 1999; O'Leary *et al*., 2002; Sim *et al*., 2002; Penderis *et al*., 2003; Ibanez *et al*., 2004; Woodruff *et al*., 2004). The presence of inhibitory molecules in myelin debris generated as a consequence of oligodendrocyte degeneration may in part provide an explanation for the so far generally frustrating failure of these different strategies (Kotter *et al*., 2006).

The key aim of our study was to examine the mechanisms that control the myelin mediated inhibition of OPC differentiation. The myelin molecules blocking OPC differentiation remain unknown. However, it is a plausible hypothesis that these molecules expressed on mature oligodendrocytes provide a feed-back inhibition for early (A2B5+) precursor cells. Under normal physiological situations this feed-back system may serve to prevent inappropriate differentiation of OPCs in normal adult white matter (Robinson and Miller, 1999), while in development one might speculate that signalling from mature oligodendrocytes to early precursors may play a functional role in regulating OPC differentiation. The situation following demyelination entails profound environmental changes as large amounts of degenerated myelin can accumulate within lesions. In experimental models this is efficiently cleared by macrophages of microglial and monocytic origin (Kotter *et al*., 2001, 2005). However, it is conceivable that if clearance of myelin debris is disturbed by alterations of the inflammatory response the presence of myelin debris can persist and thus for a prolonged period inhibit myelin repair. Recent studies suggest that remyelination requires the signalling environment provided by an acute inflammatory response (Mason *et al*., 2001; Foote and Blakemore, 2005; Kotter *et al*., 2005; Setzu *et al*., 2006). Therefore, it could be speculated that a situation may occur in which the initial inclination OPCs to differentiate is inhibited by the presence of myelin and turns into reluctance as the expression of signalling molecules required to activate OPCs diminishes.

The cascades that we found to be modulated by the presence of myelin inhibitors are similar to the ones that regulate the inhibition of axon growth via NogoR and Lingo-1 signalling (Lee *et al*., 2004; Mi *et al*., 2005). However, there is no evidence that

NogoR is expressed by OPCs and we ourselves were not able to detect NogoR expression in our cultures. While immunocytochemistry for Lingo-1 is inconclusive we found evidence of Lingo-1 mRNA in cultured OPCs (unpublished data). Furthermore, we have not seen evidence of an inhibitory effect of any of the classical myelin inhibitors of axon growth on OPC differentiation (Syed *et al*., 2008). Thus the molecular substrate present in myelin mediating the inhibitory effects remains unknown.

In this study, we developed a biochemical and proteomic protocol to identify potential candidates responsible for the myelin differentiation block. With the criteria we applied this resulted in a list of 137 myelin proteins—18 of which were previously identified using a proteomic approach. The detection of so many previously unidentified proteins in myelin can be explained in part by the biochemical separation process we developed, which removes many of the most abundant proteins. On the other hand, we applied a gel-based separation technique that is specifically tailored for the study of membrane-bound proteins that has not been previously used for the analysis of the myelin proteome. To identify the myelin protein(s) responsible for the inhibition of OPC differentiation further separation steps may be helpful. However, stringent data assessment may help to narrow down the list of potential candidates. Apart from providing a list of potential candidates our data illustrates the complexity of myelin and will provide a reference for further studies of the biology of myelin membranes.

Our results provide a model of how myelin exerts inhibitory effects on OPC differentiation. In inhibiting RhoA-ROCK and PKC(-α) signalling we have identified pharmacological targets by which OPC differentiation can be powerfully stimulated in the context of myelin inhibitors.

Fasudil is currently evaluated in a clinical setting for treatment of vasospasm as well as angina pectoris in humans (Vicari *et al*., 2005). Similarly, a number of clinical studies investigate the effects of PKC inhibitors in cancer (Mackay and Twelves, 2007). While it has to be expected that not all inhibitors can pass the brain blood barrier, a number of PKC inhibitors (e.g. Tamoxifen, Calphostin-C, HA-1004 and Ro 32-0432) (Gozal *et al*., 1998; Cerezo *et al*., 2002; Zarate *et al*., 2007) as well as Rho-cascade inhibitors (e.g. Fasudil) are able to cross the brain blood barrier (Satoh *et al*., 2008).

PKC and ROCK inhibition have shown to exert stimulating effects on neurite outgrowth in the presence of myelin inhibitors, and thus synergistic effects with respect to neural repair could be expected (Sivasankaran *et al*., 2004). As far as effects on other cell types are concerned, inhibition of PKC in microglia is associated with e.g. downregulation of MHC-II (Nikodemova *et al*., 2007), a reduction of proinflammatory cytokine, iNOS (Kang *et al*., 2001; Min *et al*., 2004), and TNF-α release (Jeohn *et al*., 2002) in response to various inflammatory modulators including LPS, ganglioside and IFNγ suggesting a reduction of proinflammatory activity in microglia. On the other hand, it has been reported that PKC inhibition lead to reduced CR3/Mac-1 and SRAI/II mediated myelin phagocytosis (Cohen *et al*., 2006) which may be relevant to myelin repair although the mechanisms we report aim at neutralizing the effects of MAI on OPC differentiation.

Astrocytes react upon PKC inhibition by e.g. decreased activation of ATP-mediated glutamate outwards channels (Rudkouskaya *et al*., 2008) and TGFb1 production (Wang *et al*., 2003), furthermore, the response to LPA is altered by a reduced proproliferative intracellular Ca2+ increase (Keller *et al*., 1997) and NGF secretion (Furukawa *et al*., 2007). It is difficult to interpret these findings in the light of remyelination as little is known about the molecular events in astrocytes during myelin repair. However, it seems unlikely that the effects of PKC inhibition on astrocytes reported will negatively impact remyelination.

Under the influence of Fasudil rat astrocytes transform *in vitro* into process bearing cells (Abe and Misawa, 2003) which can be explained by direct effects of the Rho-cascade on the cytoskeleton, on the other hand there are no data available how changes in astrocyte processes impact myelin repair.

Finally, little is known of how microglia react to inhibition of the Rho-cascade. A recent paper suggests that inhibition of RhoA by C3 induces NO and proinflammatory cytokine release, however, this is independent of ROCK signalling and was instead found to be under the control of NFkappaB suggesting that targeting down-stream signalling events may circumvent problems that may arise as a consequence of microglia activation (Hoffmann *et al*., 2008).

Our data suggest that inhibiting PKC and/or Rho-signalling would be beneficial either acutely following demyelination, where exposure to myelin debris that has yet to be cleared might critically interrupt the initiation of remyelination resulting in its long term failure or in chronic disease where OPCs remain exposed to a differentiation-inhibitory environment. The data in the current study paves the way for subsequent testing of pharmacological interventions in animal models and further clinical evaluation if the outcome were to be successful.

Supplementary material

Supplementary material is available at *Brain* online.

Acknowledgements

We especially thank Thomas Dalik for excellent technical support.

Funding

Medical University Vienna; FWF Austrian Science Funds.

References

Abe K, Misawa M. Astrocyte stellation induced by Rho kinase inhibitors in culture. Brain Res Dev Brain Res 2003; 143: 99–104.

Allen LA, Aderem A. Protein kinase C regulates MARCKS cycling between the plasma membrane and lysosomes in fibroblasts. EMBO J 1995; 14: 1109–21.

Althaus HH, Schroter J, Spoerri P, Schwartz P, Kloppner S, Rohmann A, et al. Protein kinase C stimulation enhances the process formation of

adult oligodendrocytes and induces proliferation. J Neurosci Res 1991; 29: 481–9.
Alvarez-Buylla A, Lois C. Neuronal stem cells in the brain of adult vertebrates. Stem Cells 1995; 13: 263–72.
Arbuzova A, Schmitz AA, Vergeres G. Cross-talk unfolded: MARCKS proteins. Biochem J 2002; 362: 1–12.
Asotra K, Macklin WB. Protein kinase C activity modulates myelin gene expression in enriched oligodendrocytes. J Neurosci Res 1993; 34: 571–88.
Back SA, Tuohy TM, Chen H, Wallingford N, Craig A, Struve J, et al. Hyaluronan accumulates in demyelinated lesions and inhibits oligodendrocyte progenitor maturation. Nat Med 2005; 11: 966–72.
Bansal R, Warrington AE, Gard AL, Ranscht B, Pfeiffer SE. Multiple and novel specificities of monoclonal antibodies O1, O4, and R-mAb used in the analysis of oligodendrocyte development. J Neurosci Res 1989; 24: 548–57.
Baron W, de Jonge JC, de Vries H, Hoekstra D. Regulation of oligodendrocyte differentiation: protein kinase C activation prevents differentiation of O2A progenitor cells toward oligodendrocytes. Glia 1998; 22: 121–9.
Baron W, de Vries EJ, de Vries H, Hoekstra D. Protein kinase C prevents oligodendrocyte differentiation: modulation of actin cytoskeleton and cognate polarized membrane traffic. J Neurobiol 1999; 41: 385–98.
Blakemore WF, Franklin RJ. Remyelination in experimental models of toxin-induced demyelination. Curr Top Microbiol Immunol 2008; 318: 193–212.
Byers DM, Palmer FB, Spence MW, Cook HW. Dissociation of phosphorylation and translocation of a myristoylated protein kinase C substrate (MARCKS protein) in C6 glioma and N1E-115 neuroblastoma cells. J Neurochem 1993; 60: 1414–21.
Carroll WM, Jennings AR, Ironside LJ. Identification of the adult resting progenitor cell by autoradiographic tracking of oligodendrocyte precursors in experimental CNS demyelination. Brain 1998; 121: 293–302.
Cerezo M, Laorden ML, Milanes MV. Inhibition of protein kinase C but not protein kinase A attenuates morphine withdrawal excitation of rat hypothalamus-pituitary-adrenal axis. Eur J Pharmacol 2002; 452: 57–66.
Chang A, Nishiyama A, Peterson J, Prineas J, Trapp BD. NG2-positive oligodendrocyte progenitor cells in adult human brain and multiple sclerosis lesions. J Neurosci 2000; 20: 6404–12.
Charles P, Reynolds R, Seilhean D, Rougon G, Aigrot MS, Niezgoda A, et al. Re-expression of PSA-NCAM by demyelinated axons: an inhibitor of remyelination in multiple sclerosis? Brain 2002; 125: 1972–9.
Cohen G, Makranz C, Spira M, Kodama T, Reichert F, Rotshenker S. Non-PKC DAG/phorbol-ester receptor(s) inhibit complement receptor-3 and nPKC inhibit scavenger receptor-AI/II-mediated myelin phagocytosis but cPKC, PI3k, and PLCgamma activate myelin phagocytosis by both. Glia 2006; 53: 538–50.
Colognato H, Ramachandrappa S, Olsen IM, Ffrench-Constant C. Integrins direct Src family kinases to regulate distinct phases of oligodendrocyte development. J Cell Biol 2004; 167: 365–75.
Dubois-Dalcq M, Ffrench-Constant C, Franklin RJ. Enhancing central nervous system remyelination in multiple sclerosis. Neuron 2005; 48: 9–12.
Ffrench-Constant C, Raff MC. Proliferating bipotential glial progenitor cells in adult rat optic nerve. Nature 1986; 319: 499–502.
Foote AK, Blakemore WF. Inflammation stimulates remyelination in areas of chronic demyelination. Brain 2005; 128: 528–39.
Franklin RJM. Why does remyelination fail in multiple sclerosis? Nat Rev Neurosci 2002; 3: 705–14.
Furukawa A, Kita K, Toyomoto M, Fujii S, Inoue S, Hayashi K, et al. Production of nerve growth factor enhanced in cultured mouse astrocytes by glycerophospholipids, sphingolipids, and their related compounds. Mol Cell Biochem 2007; 305: 27–34.
Garbern JY, Yool DA, Moore GJ, Wilds IB, Faulk MW, Klugmann M, et al. Patients lacking the major CNS myelin protein, proteolipid protein 1, develop length-dependent axonal degeneration in the absence of demyelination and inflammation. Brain 2002; 125: 551–61.
Gensert JM, Goldman JE. Endogenous progenitors remyelinate demyelinated axons in the adult CNS. Neuron 1997; 19: 197–203.
Gozal E, Roussel AL, Holt GA, Gozal L, Gozal YM, Torres JE, et al. Protein kinase C modulation of ventilatory response to hypoxia in nucleus tractus solitarii of conscious rats. J Appl Physiol 1998; 84: 1982–90.
Griffiths I, Klugmann M, Anderson T, Yool D, Thomson C, Schwab MH, et al. Axonal swellings and degeneration in mice lacking the major proteolipid of myelin. Science 1998; 280: 1610–3.
Hoffmann A, Hofmann F, Just I, Lehnardt S, Hanisch UK, Bruck W, et al. Inhibition of Rho-dependent pathways by Clostridium botulinum C3 protein induces a proinflammatory profile in microglia. Glia 2008; 56: 1162–75.
Horner PJ, Power AE, Kempermann G, Kuhn HG, Palmer TD, Winkler J, et al. Proliferation and differentiation of progenitor cells throughout the intact adult rat spinal cord. J Neurosci 2000; 20: 2218–28.
Ibanez C, Shields SA, El Etr M, Baulieu EE, Schumacher M, Franklin RJM. Systemic progesterone administration results in a partial reversal of the age-associated decline in CNS remyelination following toxin-induced demyelination in male rats. Neuropathol Appl Neurobiol 2004; 30: 80–9.
Jeohn GH, Cooper CL, Jang KJ, Liu B, Lee DS, Kim HC, et al. Go6976 inhibits LPS-induced microglial TNFalpha release by suppressing p38 MAP kinase activation. Neuroscience 2002; 114: 689–97.
John GR, Shankar SL, Shafit-Zagardo B, Massimi A, Lee SC, Raine CS, et al. Multiple sclerosis: re-expression of a developmental pathway that restricts oligodendrocyte maturation. Nat Med 2002; 8: 1115–21.
Kang J, Yang M, Jou I, Joe E. Identification of protein kinase C isoforms involved in interferon-gamma-induced expression of inducible nitric oxide synthase in murine BV2 microglia. Neurosci Lett 2001; 299: 205–208.
Kang S, Poliakov A, Sexton J, Renfrow MB, Prevelige PE Jr. Probing conserved helical modules of portal complexes by mass spectrometry-based hydrogen/deuterium exchange. J Mol Biol 2008; 381: 772–84.
Keller JN, Steiner MR, Holtsberg FW, Mattson MP, Steiner SM. Lysophosphatidic acid-induced proliferation-related signals in astrocytes. J Neurochem 1997; 69: 1073–84.
Kotter MR, Li WW, Zhao C, Franklin RJM. Myelin Impairs CNS remyelination by inhibiting oligodendrocyte precursor cell differentiation. J Neurosci 2006; 26: 328–32.
Kotter MR, Setzu A, Sim FJ, Van Rooijen N, Franklin RJM. Macrophage depletion impairs oligodendrocyte remyelination following lysolecithin-induced demyelination. Glia 2001; 35: 204–12.
Kotter MR, Zhao C, Van Rooijen N, Franklin RJM. Macrophage-depletion induced impairment of experimental CNS remyelination is associated with a reduced oligodendrocyte progenitor cell response and altered growth factor expression. Neurobiol Dis 2005; 18: 166–75.
Kuhlmann T, Miron V, Cuo Q, Wegner C, Antel J, Bruck W. Differentiation block of oligodendroglial progenitor cells as a cause for remyelination failure in chronic multiple sclerosis. Brain 2008; 131 (Pt 7): 1749–58.
Lappe-Siefke C, Goebbels S, Gravel M, Nicksch E, Lee J, Braun PE, et al. Disruption of Cnp1 uncouples oligodendroglial functions in axonal support and myelination. Nat Genet 2003; 33: 366–74.
Lee JK, Kim JE, Sivula M, Strittmatter SM. Nogo receptor antagonism promotes stroke recovery by enhancing axonal plasticity. J Neurosci 2004; 24: 6209–17.
Liang X, Draghi NA, Resh MD. Signaling from integrins to Fyn to Rho family GTPases regulates morphologic differentiation of oligodendrocytes. J Neurosci 2004; 24: 7140–9.
Mackay HJ, Twelves CJ. Targeting the protein kinase C family: are we there yet? Nat Rev Cancer 2007; 7: 554–62.
Mason JL, Suzuki K, Chaplin DD, Matsushima GK. Interleukin-1beta promotes repair of the CNS. J Neurosci 2001; 21: 7046–52.
McCarthy KD, de Vellis J. Preparation of separate astroglial and oligodendroglial cell cultures from rat cerebral tissue. J Cell Biol 1980; 85: 890–902.
Mi S, Miller RH, Lee X, Scott ML, Shulag-Morskaya S, Shao Z, et al. LINGO-1 negatively regulates myelination by oligodendrocytes. Nat Neurosci 2005; 8: 745–51.

Min KJ, Pyo HK, Yang MS, Ji KA, Jou I, Joe EH. Gangliosides activate microglia via protein kinase C and NADPH oxidase. Glia 2004; 48: 197–206.

Nave KA, Trapp BD. Axon-glial signaling and the glial support of axon function. Annu Rev Neurosci 2008; 31: 535–61.

Nikodemova M, Watters JJ, Jackson SJ, Yang SK, Duncan ID. Minocycline down-regulates MHC II expression in microglia and macrophages through inhibition of IRF-1 and protein kinase C (PKC)alpha/betaII. J Biol Chem 2007; 282: 15208–16.

Norton WT, Poduslo SE. Myelination in rat brain: method of myelin isolation. J Neurochem 1973; 21: 749–57.

Nunes MC, Roy NS, Keyoung HM, Goodman RR, McKhann G, Jiang L, et al. Identification and isolation of multipotential neural progenitor cells from the subcortical white matter of the adult human brain. Nat Med 2003; 9: 439–47.

O'Leary MT, Hinks GL, Franklin RJM. Increasing local levels of IGF-1 mRNA expression using adenoviral vectors does not alter oligodendrocyte remyelination in the CNS of aged rats Charlton. Mol Cell Neurosci 2002; 19: 32–42.

Osterhout DJ, Wolven A, Wolf RM, Resh MD, Chao MV. Morphological differentiation of oligodendrocytes requires activation of Fyn tyrosine kinase. J Cell Biol 1999; 145: 1209–18.

Patani R, Balaratnam M, Vora A, Reynolds R. Remyelination can be extensive in multiple sclerosis despite a long disease course. Neuropathol Appl Neurobiol 2007; 33: 277–87.

Patrikios P, Stadelmann C, Kutzelnigg A, Rauschka H, Schmidbauer M, Laursen H, et al. Remyelination is extensive in a subset of multiple sclerosis patients. Brain 2006; 129: 3165–72.

Penderis J, Woodruff RH, Lakatos A, Li WW, Dunning MD, Zhao C, et al. Increasing local levels of neuregulin (glial growth factor-2) by direct infusion into areas of demyelination does not alter remyelination in the rat CNS. Eur J Neurosci 2003; 18: 2253–64.

Reynolds BA, Weiss S. Central nervous system growth and differentiation factors: clinical horizons–truth or dare? Curr Opin Biotechnol 1993; 4: 734–8.

Riento K, Ridley AJ. Rocks: multifunctional kinases in cell behaviour. Nat Rev Mol Cell Biol 2003; 4: 446–56.

Robinson S, Miller RH. Contact with central nervous system myelin inhibits oligodendrocyte progenitor maturation. Dev Biol 1999; 216: 359–68.

Rudkouskaya A, Chernoguz A, Haskew-Layton RE, Mongin AA. Two conventional protein kinase C isoforms, alpha and betaI, are involved in the ATP-induced activation of volume-regulated anion channel and glutamate release in cultured astrocytes. J Neurochem 2008; 105: 2260–70.

Satoh S, Toshima Y, Hitomi A, Ikegaki I, Seto M, Asano T. Wide therapeutic time window for Rho-kinase inhibition therapy in ischemic brain damage in a rat cerebral thrombosis model. Brain Res 2008; 1193: 102–8.

Setzu A, Lathia JD, Zhao C, Wells K, Rao MS, Ffrench-Constant C, et al. Inflammation stimulates myelination by transplanted oligodendrocyte precursor cells. Glia 2006; 54: 297–303.

Shields SA, Gilson JM, Blakemore WF, Franklin RJM. Remyelination occurs as extensively but more slowly in old rats compared to young rats following gliotoxin-induced CNS demyelination. Glia 1999; 28: 77–83.

Sim FJ, Zhao C, Penderis J, Franklin RJM. The age-related decrease in CNS remyelination efficiency is attributable to an impairment of both oligodendrocyte progenitor recruitment and differentiation. J Neurosci 2002; 22: 2451–9.

Sivasankaran R, Pei J, Wang KC, Zhang YP, Shields CB, Xu XM, et al. PKC mediates inhibitory effects of myelin and chondroitin sulfate proteoglycans on axonal regeneration. Nat Neurosci 2004; 7: 261–8.

Stariha RL, Kim SU. Protein kinase C and mitogen-activated protein kinase signalling in oligodendrocytes. Microsc Res Tech 2001; 52: 680–8.

Stidworthy MF, Genoud S, Li WW, Leone DP, Mantei N, Suter U, et al. Notch1 and Jagged1 are expressed after CNS demyelination, but are not a major rate-determining factor during remyelination. Brain 2004; 127: 1928–41.

Syed YA, Baer AS, Lubec G, Hoeger H, Widhalm G, Kotter MR. Inhibition of oligodendrocyte precursor cell differentiation by myelin-associated proteins. Neurosurg Focus 2008; 24: E5.

Taylor CM, Pfeiffer SE. Enhanced resolution of glycosylphosphatidylinositol-anchored and transmembrane proteins from the lipid-rich myelin membrane by two-dimensional gel electrophoresis. Proteomics 2003; 3: 1303–12.

Taylor CM, Marta CB, Claycomb RJ, Han DK, Rasband MN, Coetzee T, et al. Proteomic mapping provides powerful insights into functional myelin biology. Proc Natl Acad Sci USA 2004; 101: 4643–8.

Thelen M, Rosen A, Nairn AC, Aderem A. Regulation by phosphorylation of reversible association of a myristoylated protein kinase C substrate with the plasma membrane. Nature 1991; 351: 320–2.

Thurnherr T, Benninger Y, Wu X, Chrostek A, Krause SM, Nave KA, et al. Cdc42 and Rac1 signaling are both required for and act synergistically in the correct formation of myelin sheaths in the CNS. J Neurosci 2006; 26: 10110–9.

Totoiu MO, Keirstead HS. Spinal cord injury is accompanied by chronic progressive demyelination. J Comp Neurol 2005; 486: 373–83.

Umemori H, Satot S, Yagi T, Aizawal S, Yamamoto T. Initial events of myelination involve Fyn tyrosine kinase signalling. Nature 1994; 367: 572–6.

Vanrobaeys F, VanCoster R, Dhondt G, Devreese B, VanBeeumen J. Profiling of myelin proteins by 2D-gel electrophoresis and multidimensional liquid chromatography coupled to MALDI TOF-TOF mass spectrometry. J Proteome Res 2005; 4: 2283–93.

Vicari RM, Chaitman B, Keefe D, Smith WB, Chrysant SG, Tonkon MJ, et al. Efficacy and safety of fasudil in patients with stable angina: a double-blind, placebo-controlled, phase 2 trial. J Am Coll Cardiol 2005; 46: 1803–11.

Wang CM, Chang YY, Sun SH. Activation of P2X7 purinoceptor-stimulated TGF-beta 1 mRNA expression involves PKC/MAPK signalling pathway in a rat brain-derived type-2 astrocyte cell line, RBA-2. Cell Signal 2003; 15: 1129–37.

Wang JK, Walaas SI, Sihra TS, Aderem A, Greengard P. Phosphorylation and associated translocation of the 87-kDa protein, a major protein kinase C substrate, in isolated nerve terminals. Proc Natl Acad Sci USA 1989; 86: 2253–6.

Weiss S, Dunne C, Hewson J, Wohl C, Wheatley M, Peterson AC, et al. Multipotent CNS stem cells are present in the adult mammalian spinal cord and ventricular neuroaxis. J Neurosci 1996; 16: 7599–609.

Werner HB, Kuhlmann K, Shen S, Uecker M, Schardt A, Dimova K, et al. Proteolipid protein is required for transport of sirtuin 2 into CNS myelin. J Neurosci 2007; 27: 7717–30.

Wittig I, Braun HP, Schagger H. Blue native PAGE. Nat Protoc 2006; 1: 418–28.

Wolf RM, Wilkes JJ, Chao MV, Resh MD. Tyrosine phosphorylation of p190 RhoGAP by Fyn regulates oligodendrocyte differentiation. J Neurobiol 2001; 49: 62–78.

Wolswijk G. Chronic stage multiple sclerosis lesions contain a relatively quiescent population of oligodendrocyte precursor cells. J Neurosci 1998; 18: 601–9.

Wolswijk G. Oligodendrocyte precursor cells in the demyelinated multiple sclerosis spinal cord. Brain 2002; 125: 338–49.

Wolswijk G, Noble M. Identification of an adult-specific glial progenitor cell. Development 1989; 105: 387–400.

Woodruff RA, Fruttiger M, Richardson WD, Franklin RJM. Platelet-derived growth factor regulates oligodendrocyte progenitor numbers in adult CNS and their response following CNS demyelination. Mol Cell Neurosci 2004; 25: 252–62.

Yong VW, Cheung JC, Uhm JH, Kim SU. Age-dependent decrease of process formation by cultured oligodendrocytes is augmented by protein kinase C stimulation. J Neurosci Res 1991; 29: 87–99.

Zarate CA Jr, Singh JB, Carlson PJ, Quiroz J, Jolkovsky L, Luckenbaugh DA, et al. Efficacy of a protein kinase C inhibitor (tamoxifen) in the treatment of acute mania: a pilot study. Bipolar Disord 2007; 9: 561–70.